



Synthesis and characterization of nickel(II) complexes bearing 2-(imidazol-2-yl)pyridines or 2-(pyridin-2-yl)phenanthroimidazoles/oxazoles and their polymerization of norbornene

Abiodun O. Eseola^{a,b}, Min Zhang^a, Jun-Feng Xiang^a, Weiwei Zuo^a, Yan Li^a, Joseph A.O. Woods^b, Wen-Hua Sun^{a,*}

^aKey Laboratory of Engineering Plastics and Beijing National Laboratory for Molecular Science, Institute of Chemistry, Chinese Academy of Sciences, No. 2, Beiyijie, Zhongguancun, Haidian-Sub., Beijing 100190, China

^bInorganic Chemistry Group, Department of Chemistry, University of Ibadan, Ibadan, Nigeria

ARTICLE INFO

Article history:

Received 5 January 2009

Received in revised form 15 February 2009

Accepted 19 February 2009

Available online 28 February 2009

Dedicated to Prof. R.J. Puddephatt.

Keywords:

Nickel
Catalyst
Molecular structure
Vinyl polymerization
Norbornene

ABSTRACT

Series of 2-R₁-6-(1-R₂-4,5-diphenyl-1H-imidazol-2-yl)pyridine (R₁ = R₂ = H, **L1**; R₁ = Me, R₂ = H, **L2**; R₁ = H, R₂ = Me, **L3**; R₁ = R₂ = Me, **L4**), 2-(6-R₁-pyridin-2-yl)-1H-phenanthro[9,10-d]imidazole (R₁ = H, **L5**; R₁ = Me, **L6**) and 2-(pyridin-2-yl)phenanthro[9,10-d]oxazole (**L7**) were synthesized and used to prepare their corresponding dihalonickel complexes (**C1–C9**). All organic compounds and nickel complexes were characterized by elemental and spectroscopic analyses. Molecular structures of **C1**, **C4**, **C5** and **C8** were confirmed by the single-crystal X-ray diffraction analysis. The single-crystal X-ray analysis revealed complex **C1** as a distorted octahedral geometry, complex **C4** as a distorted square pyramidal geometry, complex **C5** as a distorted trigonal bipyramidal configuration, and complex **C8** as a tetrahedral geometry. Upon activation with methylaluminumoxane (MAO), the nickel complexes showed good activity towards norbornene polymerization through main additional and minor ring-opening metathesis. The reaction parameters such as norbornene concentration, reaction temperature and different coordinate environments caused by the ligands affected their catalytic performances.

© 2009 Elsevier B.V. All rights reserved.

1. Introduction

The polymerization of norbornene (bicyclo[2.2.1]heptane) has occurred with two major mechanisms: ring-opening metathesis and vinyl addition. The ring-opening metathesis polymerization (ROMP) of norbornene was initially reported by Andersen and Merckling in 1950s [1], and has extensively investigated [2] with great achievements as part work of Noble Award in 2005 [3,4]. Vinyl polymerization of norbornene was traced back to early 1960s [5], and some efforts were made on considering their potentially advantageous properties by chemists both from industry [6] and the academia [7–11].

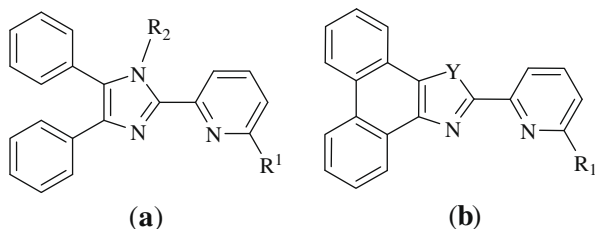
The scarcity of data such as molecular weight and molecular weight distribution of polymer presented the problem of evaluating and controlling the physical properties of polynorbornene obtained. Consequently, the case was that scientists could not measure the molecular weights and molecular weight distributions of polynorbornene obtained by vinyl polymerization. In our efforts to copolymerize ethylene with norbornene, the homopolymerization (vinyl polymerization) of norbornene only happened

with high activities by neutral salicylaldiminato nickel complexes [12] and nickel complexes bearing bis(salicylaldimine) [13] or 2-methyl-8-(diphenylphosphino)quinolines [14], and resultant polynorbornenes were measured for their molecular weights and distributions [15]. During the same period and before, there were some works employing nickel complexes as catalysts for vinyl polymerization of norbornene without measuring the molecular weights of polynorbornene obtained by GPC [16–18]. It would be fair to mention that the polynorbornenes obtained by titanium complex catalysts were reported with molecular weights and distributions in the same period [19].

Inspired by these achievements, search for new nickel complexes as catalysts for norbornene polymerization has become a hot topic in our [20–24] and other groups [25–29]. After we solved the problem of reactor fouling by supporting nickel catalysts on spherical MgCl₂ [30], we attended to their properties and application. Unfortunately, there is no melting point observable for such polymers. Therefore, further papers were not submitted even though an invited lecture was delivered [31].

Recently, it was reported that norbornene polymerization catalyzed by some iridium complexes proceeded by both ROMP and vinyl-polymerization styles [32,33]. Such phenomenon has also been described for cobalt [34] and palladium [35] precursors. However,

* Corresponding author. Tel.: +86 10 62557955; fax: +86 10 62618239.
E-mail address: whsun@iccas.ac.cn (W.-H. Sun).



Scheme 1. Ligand frameworks in this work.

it is taken for granted that norbornene polymerization mediated by nickel systems involves only vinyl-type polymerization mode. The occurrences of the two active species for polymerization may lead to bimodal molecular weight distributions [36], but bimodal distributions could also result from pure vinyl polymerization in the presence of different active site types [29].

Though the recent progress made on nickel catalytic system, it is usual to explore nickel complexes for their catalytic behaviours regardless of whether they are more active than literature findings. This is so because academic understanding on polymerization mechanisms and the nature of the active species in relation to activity trends is still largely lacking. One of the few reported conclusions, ‘trigger’ mechanism [37], proposed that norbornene monomer always occupies coordination site on active species, and that the complexed norbornene monomer will only undergo incorporation into the polymer chain via Ni–C *cis-exo* insertion only if triggered by a new monomer that is accessing the active site. Therefore, it is conceivable that productivity and polymer molecular weight should increase at increasing temperatures and/or increasing monomer concentrations. Such a trend is observed for some nickel complexes (e.g. anilido–imino nickel complexes [29]), but may be inadequate to explain active site characteristics for higher catalytic activities and polymer molecular weight increase that is favoured at reducing temperatures. Moreover, the blocked polynorbornenes are expected for making parts without constrained rings in order to have the polymer chains foldable and possible for their melting points of such polymers. In our on going syntheses of 2-(4,5-diphenyl-imidazol-2-yl)pyridines (**a**) or 2-(pyridin-2-yl)phenanthroimidazoles/oxazoles (**b**) (Scheme 1), their corresponding dihalonickel complexes showed good activities toward norbornene polymerization, in which polynorbornenes have some remaining double bonds and indicate the polymerization through major additional and minor ring-opening metathesis. Herein we report syntheses, characterization and norbornene polymerization behaviour of dihalonickel complexes based on pyridine derivatives such as 2-(imidazol-2-yl)pyridines or 2-(pyridin-2-yl)phenanthroimidazoles/oxazoles (Scheme 2).

2. Experimental

All air- or moisture-sensitive manipulations were carried out under an atmosphere of nitrogen using standard Schlenk techniques. IR spectra were obtained on a Perkin–Elmer FT-IR 2000 spectrophotometer by using KBr disks in the range of 4000–400 cm^{-1} . NMR spectra were recorded with a Bruker ARX 400 spectrometer with TMS as the internal standard. Solid state ^{13}C spectra were obtained on a Bruker AVANCE III 400 WB spectrometer by using *cpdross* pulse program, in which the delay time is 3 s and the spectra are accumulated for 1024 scans with spinning rate is 5 kHz. Elemental analysis was carried out using a Flash EA 1112 microanalyzer. Toluene was refluxed over sodium-benzophenone and distilled under nitrogen prior to use. Methylaluminoxane (MAO, 1.46 M in toluene) was purchased from Akzo Nobel Corp. Norbornene (bicyclo-[2.2.1]hept-2-ene; Acros) was refluxed over sodium for 12 h and distilled under nitrogen, and applied as toluene solution. All other chemicals are commercially available and used without further purification unless stated otherwise.

3. Synthesis of pyridine derivatives and nickel complexes

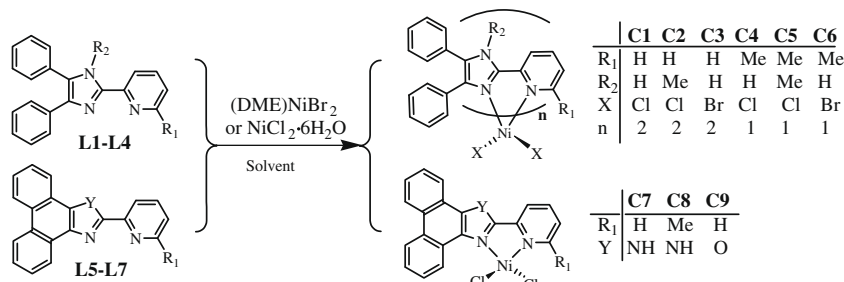
3.1. Synthesis of pyridine derivatives (L1–L7)

3.1.1. 2-(4,5-Diphenyl-1H-imidazol-2-yl)pyridine (L1)

Benzil (3.00 g, 14.27 mmol) and ammonium acetate (11.00 g, 0.14 mol) were put into a flask and after filling with nitrogen, 20 mL each of ethanol and dichloromethane were added. While stirring at reflux, 2-pyridinecarboxaldehyde (1.6 mL, 17.12 mmol) was added followed by catalytic amount of glacial acetic acid (0.5 mL) and 2 h reflux. The reaction solution was cooled, extracted three times with 100 mL portions of dichloromethane, and the combined extracts were washed with 10 mL water, dried and purified on silica gel column with petroleum ether/ethyl acetate/dichloromethane (10:1:1) as eluent. Compound **L1** was isolated as white crystalline solid (0.85 g, 20.7%). Melting point (M.p.) 174–176 °C. Selected IR peaks (KBr disc, cm^{-1}): ν 3050vs, 1601s, 1590s, 1581s, 1567s, 1475vs, 768s, 739s, 697vs. ^1H NMR (400 MHz, TMS, CDCl_3): δ 10.56(s, br, 1H); 8.51(d, $J = 4.8$ Hz, 1H); 8.29(d, $J = 8.0$ Hz, 1H); 7.78(dd, $J = 7.6$ Hz, 1H); 7.76(s, br, 2H); 7.49(s, br, 2H); 7.34(m, br, 6H), 7.22(dd, $J = 5.0$ Hz, 1H). ^{13}C NMR (100 MHz, TMS, CDCl_3): 148.7, 148.2, 145.4, 137.1, 128.6, 127.9, 123.2, 120.1. *Anal. Calc.* for $\text{C}_{20}\text{H}_{15}\text{N}_3$: C, 80.78; H, 5.08; N, 14.13. Found; C, 80.99; H, 5.01; N, 14.38%.

3.1.2. 2-Methyl-6-(4,5-diphenyl-1H-imidazol-2-yl)pyridine (L2)

Benzil (2.06 g, 9.78 mmol), 6-methyl-2-pyridinecarboxaldehyde (1.18 g, 9.78 mmol), ammonium acetate (7.0 g, 90.81 mmol) and catalytic amount of glacial acetic acid (1 mL) were treated in the same manner as for compound **L1** above, except that petroether/ethyl acetate/dichloromethane (2:2:1) was employed for column



Scheme 2. General synthetic routes to the complexes C1–C9.

chromatography. The imidazole product (**L2**) was isolated as white solid (1.44 g, 47.3% yield). M.p. 198–200 °C. Selected IR peaks (KBr disc, cm^{-1}): ν 3061s, 2959s, 1597s, 1572s, 1501m, 1474vs, 1454vs, 765vs, 697vs. ^1H NMR (400 MHz, TMS, CDCl_3): δ 10.50(s, br, 1H); 8.09(d, $J = 7.8$ Hz, 1H); 7.67(m, 3H); 7.50(br, d, $J = 5.9$ Hz, 2H); 7.32(m, br, 6H); 7.09(d, $J = 7.6$ Hz, 1H); 2.61(s, 3H). ^{13}C NMR (100 MHz, TMS, CDCl_3): 157.7, 147.5, 145.5, 137.4, 128.5, 127.9, 127.1, 122.8, 117.1, 24.2. *Anal. Calc.* for $\text{C}_{21}\text{H}_{17}\text{N}_3$: C, 81.00; H, 5.50; N, 13.49. Found: C, 80.56; H, 5.59; N, 13.86%.

3.1.3. 2-(1-Methyl-4,5-diphenyl-1H-imidazol-2-yl)pyridine (**L3**)

In acetone (30 mL), 2-(4,5-diphenyl-1H-imidazol-2-yl)pyridine (0.44 g, 1.47 mmol) and K_2CO_3 (0.41 g, 2.95 mmol) were refluxed for 30 min. On cooling, iododomethane (0.13 mL, 2.06 mmol) was added and the reaction mixture stirred at room temperature for 24 h. Removal of solvent under vacuum followed by addition of about 50 mL water gave white particles which were filtered, washed with water and dried. This was purified on silica gel column with ethyl acetate/petroleum ether (1:5) to obtain compound **L3** (0.34 g, 71.4%). M.p. 121–123 °C. Selected IR peaks (KBr disc, cm^{-1}): ν 3104m, 3034m, 2953w, 1606s, 1573m, 799s, 700vs. ^1H NMR (400 MHz, TMS, CDCl_3): δ 8.62(d, $J = 4.8$ Hz, 1H); 8.32(d, $J = 8.0$ Hz, 1H); 7.81(dd, $J = 7.7$ Hz, 1H); 7.55(d, $J = 7.2$ Hz, 2H); 7.48(m, 3H); 7.41(m, 2H); 7.24(m, 1H); 7.22(dd, $J = 7.2$ Hz, 2H); 7.16(d, 7.2 Hz, 1H); 3.91(s, 3H). ^{13}C NMR (100 MHz, TMS, CDCl_3): 151.0, 148.3, 145.0, 137.9, 136.6, 134.7, 132.2, 131.0, 129.0, 128.7, 128.1, 126.9, 126.4, 123.7, 122.5, 34.1. *Anal. Calc.* for $\text{C}_{21}\text{H}_{17}\text{N}_3$: C, 81.00; H, 5.50; N, 13.49. Found: C, 81.03; H, 5.52; N, 13.32%.

3.1.4 2-Methyl-6-(1-methyl-4,5-diphenyl-1H-imidazol-2-yl)pyridine (**L4**)

In 30 mL solvent, the reactants 2-methyl-6-(4,5-diphenyl-1H-imidazol-2-yl)pyridine (0.44 g, 1.40 mmol), K_2CO_3 (0.39 g, 2.79 mmol) and methyl iodide (0.12 mL, 1.95 mmol) were subjected to similar procedure as for compound **L3** to obtain compound **L4** (0.27 g, 66.1%). M.p. 120–122 °C. Selected IR peaks (KBr disc, cm^{-1}): ν 3100m, 3056w, 3030w, 2987w, 1604s, 1573s, 790vs. ^1H NMR (400 MHz, TMS, CDCl_3): δ 8.08(d, $J = 7.8$ Hz, 1H); 7.69(dd, $J = 7.8$ Hz, 1H); 7.53(d, $J = 7.3$ Hz, 2H); 7.46(m, 3H); 7.40(m, 2H); 7.21(dd, $J = 7.2$ Hz, 2H); 7.13(dd, $J = 7.6$ Hz, 2H); 3.88(s, 3H); 2.60(s, 3H). ^{13}C NMR (100 MHz, TMS, CDCl_3): 157.1, 150.3, 145.2, 137.8, 137.0, 134.7, 132.0, 131.1, 131.0, 129.0, 128.6, 128.1, 127.0, 126.3, 122.0, 120.7, 34.0, 24.5. *Anal. Calc.* for $\text{C}_{22}\text{H}_{19}\text{N}_3$: C, 81.20; H, 5.89; N, 12.91. Found: C, 81.36; H, 5.92; N, 12.78%.

Compounds **L5–L7** were also obtained by similar procedure for preparation of compound **L1**. The general procedure is as follows: Phenanthrenequinone and the corresponding aldehyde (1 M equiv.) were refluxed for 3 h in the presence of ammonium acetate (10 M equiv.) and glacial acetic acid (0.5–1.0 mL) as catalyst. The reaction solution was cooled and stirred with a few drops of concentrated aqueous ammonia at room temperature to neutralize residual acid. The mixture was extracted 2ce with dichloromethane (60 mL and 20 mL) and the combined organic extract concentrated under vacuum was purified on silica gel column using petroleum ether/dichloromethane (1:4) as eluent. The eluent portions containing the respective products were collected and concentrated under vacuum. Addition of petroleum ether precipitated the products which were filtered washed with petroleum ether and dried under vacuum at 60 °C. Reaction and analytical data for the respective ligands are as follows.

3.1.5. 2-(Pyridin-2-yl)-1H-phenanthro[9,10-d]imidazoles (**L5**)

Obtained 0.48 g, 11.3%. M.p. 200–202 °C. Selected IR peaks (KBr disc, cm^{-1}): ν 3434vs, 3052s, 1614w, 1594vs, 1566s, 1455vs, 1445vs, 1426s, 1396m, 1234s, 1144m, 788s, 758vs, 725vs. ^1H NMR (CDCl_3 , 400 MHz, TMS): 11.34(s, br, 1H); 8.73(s, br, 3H);

8.64(d, $J = 4.8$ Hz, 1H); 8.53(d, $J = 8.0$ Hz, 1H); 8.08(s, br, 1H); 7.89(dd, 7.7 Hz, 1H); 7.71(s, br, 2H); 7.64(m, 2H); 7.34(dd, $J = 4.9$ Hz, 1H). ^{13}C NMR (CDCl_3 , 100 MHz, TMS): 149.02, 148.57, 148.38, 137.31, 127.08, 125.61, 123.90, 121.18. *Anal. Calc.* for $\text{C}_{20}\text{H}_{13}\text{N}_3 \cdot 0.25\text{H}_2\text{O}$: C, 80.11; H, 4.54; N, 14.01. Found: C, 79.60; H, 4.63; N, 14.14%.

3.1.6. 2-(6-Methylpyridin-2-yl)-1H-phenanthro[9,10-d]imidazoles (**L6**)

Obtained 0.61 g, 41.0%. M.p. 218–220 °C. Selected IR peaks (KBr disc, cm^{-1}): ν 3435s, 3072s, 1615m, 1595s, 1573vs, 1516m, 1461vs, 1450vs, 1427vs, 1235s, 1120m, 1038s, 796s, 752vs, 723vs. ^1H NMR (CDCl_3 , 400 MHz, TMS): 11.45(s, br, 1H); 8.74(m, 3H); 8.34(d, $J = 7.8$ Hz, 1H); 8.12(d, $J = 6.4$ Hz, 1H); 7.76(m, 2H), 7.64(m, 3H); 7.20(d, $J = 7.3$ Hz, 1H); 2.66(s, 3H). ^{13}C NMR (CDCl_3 , 100 MHz, TMS): 158.1, 148.5, 147.8, 137.5, 128.6, 127.1, 125.5, 123.6, 122.5, 118.2, 24.31. *Anal. Calc.* for $\text{C}_{21}\text{H}_{15}\text{N}_3 \cdot 0.9\text{H}_2\text{O}$: C, 76.62; H, 5.27; N, 12.77. Found: C, 76.65; H, 5.18; N, 12.79%.

3.1.7. 2-(Pyridin-2-yl)phenanthro[9,10-d]oxazole (**L7**)

Obtained 2.50 g, 58.6%. M.p. 199–201 °C. Selected IR peaks (KBr disc, cm^{-1}): ν 3056m, 1615m, 1589vs, 1566s, 1455vs, 1425vs, 1251s, 1234s, 1082vs, 757vs, 724vs. ^1H NMR (CDCl_3 , 400 MHz, TMS): 8.89(d, $J = 4.8$ Hz, 1H); 8.73(m, 3H); 8.47(m, 2H); 7.94(dd, $J = 7.6$ Hz, 1H), 7.73(m, 4H); 7.46(dd, $J = 4.8$ Hz, 1H). ^{13}C NMR (CDCl_3 , 100 MHz, TMS): 160.7, 150.4, 146.4, 145.7, 137.1, 135.6, 129.9, 129.2, 127.9, 127.4, 126.9, 126.4, 126.2, 125.0, 123.8, 123.5, 123.2, 123.1, 121.4, 121.1. *Anal. Calc.* for $\text{C}_{20}\text{H}_{12}\text{N}_2\text{O}$: C, 81.07; H, 4.08; N, 9.45. Found: C, 80.84, H, 4.20, N, 9.41%.

3.2. Syntheses of Ni(II) complexes **C1–C9**

3.2.1. Complex **C1** ($\text{L1}_2\text{NiCl}_2$)

The dichloromethane (10 mL) solution of **L1** (0.13 g, 0.45 mmol) was added in drops to a stirring solution of $\text{NiCl}_2 \cdot 6\text{H}_2\text{O}$ (54.0 mg, 0.225 mmol) in ethanol (6 mL) at room temperature. The stirring continued for 12 h after which the resultant particles were filtered to give **C1** as light blue micro-crystals (0.13 g, 73.4%). Decomposition point (D.p.) >302 °C. Selected IR peaks (KBr, cm^{-1}): ν 3285m, 3055vs, 1615vs, 1585vs, 1573s, 1535s, 1475vs, 1459vs, 774vs, 696vs. *Anal. Calc.* for $\text{C}_{41}\text{H}_{36}\text{Cl}_2\text{N}_6\text{NiO}_2$: C, 63.59; H, 4.69; N, 10.85. Found: C, 63.30; H, 4.66; N, 10.58%.

3.2.2. Complex **C2** ($\text{L3}_2\text{NiCl}_2$)

$\text{NiCl}_2 \cdot 6\text{H}_2\text{O}$ (46.0 mg, 0.20 mmol) and **L3** (0.12 g, 0.40 mmol) were reacted in a similar manner as for **C1** to obtain **C2** as a blue powder (0.15 g, 85.2%). D.p. >394 °C. Selected IR peaks (KBr, cm^{-1}): ν 3104m, 3034m, 2953w, 1606s, 1573m, 799s, 700vs. *Anal. Calc.* for $\text{C}_{42}\text{H}_{36}\text{Cl}_2\text{N}_6\text{NiO}$: C, 65.48; H, 4.71; N, 10.91. Found: C, 65.54; H, 4.53; N, 10.87%.

3.2.3. Complex **C3** ($\text{L1}_2\text{NiBr}_2$)

To a THF (2 mL) solution of $(\text{DME})\text{NiBr}_2$ (90.0 mg, 0.29 mmol), the THF (4 mL) solution of **L1** (0.19 g, 0.64 mmol) was added in drops and stirring continued for 12 h at room temperature. Diethyl ether (5 mL) was added to precipitate the blue powder, which was filtered, washed with THF/diethyl ether mixture, and dried under vacuum to give **C3** as blue powder (0.24 g, 78.8%). D.p. >312 °C. Selected IR peaks (KBr, cm^{-1}): ν 3433m(br), 3321m, 3106s, 3056s, 3009m, 1614s, 1584m, 1574m, 1507m, 773s, 695vs. *Anal. Calc.* for $\text{C}_{40}\text{H}_{34}\text{Br}_2\text{N}_6\text{NiO}_2$: C, 56.57; H, 4.04; N, 9.90. Found: C, 56.46; H, 3.79; N, 9.47%.

3.2.4. Complex **C4** (L2NiCl_2)

$\text{NiCl}_2 \cdot 6\text{H}_2\text{O}$ (0.15 g, 0.65 mmol) and **L2** (0.20 g, 0.65 mmol) were reacted in a similar manner as for **C1** to obtain **C4** as a yellow

powder (0.26 g, 91.2%). D.p. >216 °C. Selected IR peaks (KBr, cm^{-1}): ν 3348s (br), 3066vs, 1615m, 1603m, 1568s, 1478vs, 1247s, 805s, 765s, 694vs. *Anal. Calc.* for $\text{C}_{21}\text{H}_{19}\text{Cl}_2\text{N}_3\text{NiO}$: C, 54.95; H, 4.17; N, 9.15. Found: C, 54.74; H, 4.24; N, 8.62%.

3.2.5. Complex **C5** (L4NiCl_2)

$\text{NiCl}_2 \cdot 6\text{H}_2\text{O}$ (0.1 g, 0.40 mmol) and **L4** (0.13 g, 0.40 mmol) were reacted in a similar manner as for **C1** to obtain **C5** as a yellow powder (0.16 g, 88.2%). D.p. >214 °C. Selected IR peaks (KBr, cm^{-1}): ν 3100m, 3056w, 3030w, 2987w, 1604s, 1573s, 790vs. *Anal. Calc.* for $\text{C}_{22}\text{H}_{19}\text{Cl}_2\text{N}_3\text{Ni} \cdot (1/2)\text{H}_2\text{O}$: C, 56.95; H, 4.34; N, 9.06. Found: C, 56.88; H, 4.18; N, 9.11%.

3.2.6. Complex **C6** (L2NiBr_2)

(DME) NiBr_2 (0.28 g, 0.92 mmol) in THF (2 mL) and **L2** (0.32 g, 1.02 mmol) were reacted according to procedure for preparation of **C1** to give **C6** as yellow cake (0.50 g, 95.3%). D.p. >220 °C. Selected IR peaks (KBr, cm^{-1}): ν 3435s(br), 3160m, 3138m, 3064m, 2978m, 2874m, 1616s, 1566s, 806s, 695vs. *Anal. Calc.* for $\text{C}_{21}\text{H}_{17}\text{Br}_2\text{N}_3\text{Ni} \cdot (1/2)(\text{C}_2\text{H}_5)_2\text{O}$: C, 48.73; H, 3.91; Br, 28.19; N, 7.4. Found: C, 48.80; H, 3.92; N, 6.96%.

3.2.7. Complex **C7** (L5NiCl_2)

Compound **L5** (0.13 g, 0.43 mmol) taken up in dichloromethane (10 mL) was added in drops and at room temperature to a stirring solution of $\text{NiCl}_2 \cdot 6\text{H}_2\text{O}$ (0.10 g 0.43 mmol) in ethanol (6 mL). The stirring continued for 12 h after which the reaction solution was diluted with diethyl ether and the resultant light green powder filtered. The product was washed with diethyl ether and dried under vacuum at 60 °C to obtain **C7** (0.33 g, 78.1%). D.p. 402 °C. Selected IR peaks (KBr disc, cm^{-1}): ν 3363, 3096, 3039, 1608, 1521, 1455,

1445, 1428, 1299, 1161, 788, 750, 718. *Anal. Calc.* for $\text{C}_{20}\text{H}_{13}\text{Cl}_2\text{N}_3\text{Ni} \cdot \text{H}_2\text{O}$: C, 54.23; H, 3.41; N, 9.49. Found: C, 54.30; H, 3.17; N, 9.37%.

3.2.8. Complex **C8** (L6NiCl_2)

Compound **L6** (0.10 g, 0.32 mmol) and $\text{NiCl}_2 \cdot 6\text{H}_2\text{O}$ (76.8 mg, 0.32 mmol) were reacted in the same manner as for complex **C1** above to obtain **C8** as a yellow powder (0.12 g, 87.9%). D.p. >390 °C. Selected IR peaks (KBr disc, cm^{-1}): ν 3045m, 2950m, 1654m, 1591vs, 1491vs, 1279s, 775vs, 711s. *Anal. Calc.* for $\text{C}_{21}\text{H}_{19}\text{Cl}_2\text{N}_3\text{NiO}_2$: C, 53.10; H, 4.03; N, 8.85. Found: C, 52.75; H, 3.49; N, 8.50%.

3.2.9. Complex **C9** (L7NiCl_2)

Compound **L7** (0.20 g, 0.68 mmol) and $\text{NiCl}_2 \cdot 6\text{H}_2\text{O}$ (0.16 g, 0.68 mmol) were reacted in the same manner as for complex **C1** above to afford **C9** as light green powder (0.26 g, 90.4%). D.p. >422 °C. Selected IR peaks (KBr disc, cm^{-1}): ν 3483s, 3302vs(br), 3074m, 1638vs, 1615s, 1543vs, 1478s, 1439vs, 1292s, 1167s, 788s, 759vs. *Anal. Calc.* for $\text{C}_{20}\text{H}_{12}\text{Cl}_2\text{N}_2\text{NiO} \cdot (1/2)\text{H}_2\text{O}$: C, 55.23; H, 3.01; N, 6.44. Found: C, 55.50; H, 3.77; N, 6.36%.

4. Polymerization of norbornene

In the polymerization experiment, the general procedure is as follows: the catalyst (2.0 μmol Ni) was weighed into Schlenk-type glassware, charged with nitrogen and the appropriate volume of norbornene solution in toluene was added via syringe through a rubber septum. Necessary amount of toluene was added to reactor to achieve the total reaction volume, which was typically 10 mL. Polymerization reaction was initiated by addition of corresponding volume of 1.46 M solution of MAO in toluene. After respective

Table 1

Crystal data for processing parameters for **C1**, **C4**, **C5** and **C8**.

	C1 · CH_3OH	C4 · $2\text{CH}_3\text{OH}$	C5	C8 · DMF
Formula	$\text{C}_{40}\text{H}_{30}\text{N}_6\text{NiCl}_2 \cdot \text{CH}_3\text{OH}$	$\text{C}_{21}\text{H}_{17}\text{N}_3\text{NiCl}_2 \cdot 2\text{CH}_3\text{OH}$	$\text{C}_{22}\text{H}_{19}\text{N}_3\text{NiCl}_2$	$\text{C}_{21}\text{H}_{15}\text{N}_3\text{NiCl}_2 \cdot \text{DMF}$
Formula weight	756.33	505.07	455.01	512.07
T (K)	173(2)	173(2)	173(2)	173(2)
Wavelength (Å)	0.71073	0.71073	0.71073	0.71073
Crystal system	triclinic	monoclinic	triclinic	monoclinic
Space group	$P\bar{1}$	$P2(1)/n$	$P\bar{1}$	$P2(1)/n$
a (Å)	11.933(2)	10.665(2)	8.4913(2)	13.437(3)
b (Å)	12.526(3)	9.794(2)	11.359(2)	9.7111(2)
c (Å)	15.126(3)	22.088(4)	12.622(3)	18.033(4)
α (°)	102.72(3)	90	66.09(3)	90
β (°)	96.03(3)	91.05(3)	86.66(3)	108.43(3)
γ (°)	116.59(3)	90	70.65(3)	90
V (Å ³)	1917.7(7)	2306.8(8)	1046.0(4)	2232.4(8)
Z	2	4	2	4
D_{calc} (g m^{-3})	1.310	1.454	1.445	1.524
μ (mm^{-1})	0.685	1.098	1.195	1.134
F(000)	784	1048	468	1056
Crystal size (mm)	$0.46 \times 0.46 \times 0.29$	$0.42 \times 0.26 \times 0.24$	$0.10 \times 0.10 \times 0.10$	$0.53 \times 0.47 \times 0.28$
θ Range (°)	1.42–25.00	2.14–25.00	2.08–25.00	1.66–27.39
Limiting indices	$-14 \leq h \leq 14$ $-14 \leq k \leq 14$ $-17 \leq l \leq 17$	$-12 \leq h \leq 12$ $-11 \leq k \leq 11$ $-26 \leq l \leq 26$	$-10 \leq h \leq 10$ $-13 \leq k \leq 13$ $-14 \leq l \leq 14$	$-17 \leq h \leq 17$ $-12 \leq k \leq 12$ $-23 \leq l \leq 23$
Number of reflections collected	12553	12132	6844	9623
Number of unique reflections	6744	4054	3683	5079
R(int)	0.0311	0.0577	0.0279	0.0265
Completeness to θ (%)	99.9 ($\theta = 25.00$)	99.6 ($\theta = 25.00$)	99.9 ($\theta = 25.00$)	99.8 ($\theta = 27.39$)
Number of parameters	464	289	254	300
Goodness-of-fit (GOF) on F^2	1.152	1.337	1.130	1.352
Final R indices ($I > 2\sigma(I)$)	$R_1 = 0.0507$ $wR_2 = 0.1031$	$R_1 = 0.0607$ $wR_2 = 0.1087$	$R_1 = 0.0555$ $wR_2 = 0.1167$	$R_1 = 0.0622$ $wR_2 = 0.1276$
R indices (all data)	$R_1 = 0.0647$ $wR_2 = 0.1074$	$R_1 = 0.0728$ $wR_2 = 0.1126$	$R_1 = 0.0688$ $wR_2 = 0.1222$	$R_1 = 0.0795$ $wR_2 = 0.1382$
Largest difference in peak and hole ($e \text{ \AA}^{-3}$)	0.657, -0.457	0.559, -0.763	1.019, -0.561	0.438, -0.506

durations, the polymerization was terminated by pouring into 100 mL acidic ethanol (ethanol:conc. HCl = 95:5). The polymer was isolated by filtration, washed with ethanol, and dried in vacuum at 60 °C overnight. All polynorbornenes showed the almost same IR spectra. IR (KBr disc, cm^{-1}): 2945 (vs), 2867 (vs), 1477 (m), 1452 (s), 1374 (w), 1294 (m), 1257 (m), 1222 (w), 1146 (m), 1108 (w), 1084 (w), 1022 (w), 939 (m), 891 (m), 739 (s), 702 (w), 648(w).

4.1. X-ray crystallographic studies

Single-crystal X-ray diffraction studies for complexes **C1**, **C4**, **C5** and **C8** were done on a Rigaku R-AXIS Rapid IP diffractometer with graphite monochromated Mo K α radiation ($\lambda = 0.71073 \text{ \AA}$). Intensities were corrected for Lorentz and polarization effects and empirical absorption. A direct method was applied in solving the structural data and refinement done by full-matrix least-squares on F^2 . All non-hydrogen atoms were refined anisotropically. All hydrogen atoms were placed in calculated positions except for the imidazole and DMF carbonyl protons which were assigned based on identified peak positions during refinement. Structure solution and refinement were performed using the SHELXL-97 package [45]. Crystal data and processing parameters for **C1**, **C4**, **C5** and **C8** are presented in Table 1.

5. Results and discussions

5.1. Syntheses of pyridine derivatives (**L1**–**L7**)

Using modified literature method [38], the imidazole ligands (**L1**, **L2**, **L5** and **L6**) and an oxazole analogue (**L7**) were synthesized in appreciable to good yields by refluxing the respective α -diones, appropriate pyridinecarboxaldehyde and ten fold ammonium acetate in ethanol/dichloromethane solvent mixture (1:1, v/v) in the presence of catalytic amount of glacial acetic acid. Bearing in mind the intention to tune the electronic properties of the imidazole ring, **L3** and **L4** were prepared in good yields by respective methylation of 1-imidazole position on **L1** and **L2** using K_2CO_3 as base and CH_3I as alkylating agent in acetone. All the obtained compounds were fully characterized by IR, ^1H NMR, ^{13}C NMR and elemental analyses. According to the method of Steck and Day [38], preparation of imidazoles by coupling α -diones with aldehydes in the presence of excess ammonium acetate is usually conducted by refluxing in glacial acetic acid serving the dual purpose of solvent as well as reaction catalyst. Attempts to prepare **L1**, **L2** and **L5**–**L7** in glacial acetic acid as solvent usually gave a mixture of many products and no appreciable amount of the target ligands even when conducted under nitrogen protection. To the best of our knowledge, detailed synthetic protocol is unavailable for oxazole and/or imidazole ring synthesis by condensation of α -diones with aldehyde-substituted pyridines. Our careful examination of ^1H NMR data for the only known condensation attempt reveals that the oxazole derivative was obtained, but was thought to be and reported as the target imidazole ligand [39]. Attempt to use either ethanol or dichloromethane as a single solvent reaction system gave insignificant yields obviously because of difference in solubility of benzil or phenanthrene on the one hand and ammonium acetate on the other hand. Phenanthrenequinone formed both oxazole (major) and imidazole products. However, the oxazole analogue was not noticed when benzil was employed as reactant under similar reaction action conditions. This can be rationalized from the close proximity and alignment of the two carbonyl groups in phenanthrenequinone relative to that in benzil, which has O–O dihedral angle as large as 90° [40]. Cyclic coupling of N–O phenanthrene intermediates with the aldehyde moieties is, thus, suggested to oc-

cur in a faster step relative to formation of the N–N species. Similar mechanism was upheld by Stein and Day [41].

5.2. Syntheses of the Ni(II) complexes

All nickel complexes were obtained in good yields by routinely reacting appropriate ratios of $\text{NiCl}_2 \cdot 6\text{H}_2\text{O}$ or (DME) NiBr_2 to the respective ligands at room temperature. They were characterized by FT-IR and elemental analyses. Peaks assignable to the C=N double bonds were shifted to lower wavenumbers in the complexes compared to the ligand IR peak positions for similar vibrations. Single-crystal X-ray diffraction experiments were performed for **C1**, **C4**, **C5** and **C8**. Attempts to prepare the mono-ligated analogues of **C1**, **C2** and **C3** proved abortive as we observed that coordination of **L1** and **L3** with nickel halides displayed a preference for the bis-ligand structures even when deliberate slight excess of nickel salt was experimented. It is note worthy that all the case of bis-chelated nickel complexes were distinguishable by their characteristic blue color and higher CHN values of elemental analyses (EA) in contrast to the bright yellow shades of mono-ligated complexes **C4**, **C5** and **C6** with lower EA values. It is also observable that all bis-coordinated compounds resulted from ligands without ortho-methyl group to the pyridyl nitrogen, which probably hindered the phenomenon in the instances of complexes derived from **L2** and **L4**. In general, this phenomenon suggests the importance of its steric influence of the ligand system. In contrast, the phenanthro-substituted ligands conformed to 1:1 complexation regardless of whether R_1 is methyl or proton. Therefore, it is considered that the constrained ring of phenanthro-ring play roles in such coordination.

5.3. Molecular structure of complexes

Single crystals of **C1** suitable for X-ray diffraction were grown by slow diffusion of diethyl ether into its methanol solution. The molecular structure is shown in Fig. 1. The distorted octahedral coordination environment of complex **C1** consists of two units of ligand **L1**, one chloride and an oxygen atom from adducted methanol group. The chelating ligands provided four N atoms such that the two pyridyl rings are *trans*-displaced ($\text{N1-Ni(1)-N4} = 175.66(9)^\circ$) while the imidazolyl nitrogen donors are *cis*-placed ($\text{N2-Ni-N5} = 84.30^\circ$). The chloride and oxygen atoms are located *cis*- to each other and form an approximate right angle ($84.32(9)^\circ$). The second chloride anion is detached from metal center and located within the crystal lattice mediating H-bond networks. The Ni–N bond lengths ($\text{Ni(1)-N1} = 2.095(3) \text{ \AA}$, $\text{Ni(1)-N2} = 2.095(3) \text{ \AA}$), which are equal, $\text{Ni(1)-Cl1} = 2.4668(9) \text{ \AA}$ and $\text{Ni(1)-O1} = 2.071(3) \text{ \AA}$ are similar to those nickel analogues observed in the literatures [42–44], and in the typical range for nickel complexes. In each ligand, the pyridyl and imidazolyl ring together with the chelating ring are almost in the same plane, while dihedral angles between the substituent phenyl groups and the five-membered ring randomly varied; planes ($\text{C9-C10-C11-C12-C13-C14}$) and ($\text{C15-C16-C17-C18-C19-C20}$) of one ligand unit formed dihedral angles of 71.2° and 14.6° , respectively, with their imidazole ring (N2-C6-N3-C8-C7), while planes ($\text{C49-C50-C48-C47-C46-C45}$) and ($\text{C39-C44-C43-C42-C41-C40}$) of the second ligand unit formed dihedral angles 43.1° and 30.1° with their imidazole plane (N6-C36-C38-C37-N5), respectively.

The steric demands caused by ortho-substituent methyl group on the pyridyl ring lead to mono-ligand structures. From the ORTEP plot of **C4** (Fig. 2), the Ni center can best be described as square pyramidal. The square plane consists of the *trans*-chloride atoms, pyridyl N(1) and O(1) of coordinated methanol and the angles between diagonals of the tetragonal plane are all close to right angles: $\text{N(1)-Ni(1)-Cl(2)} = 91.02(9)$; $\text{N(1)-Ni(1)-Cl(1)} = 86.79(9)$;

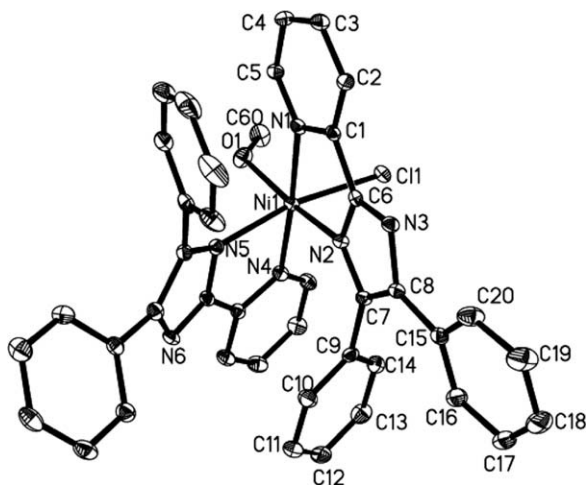


Fig. 1. Molecular structure of complex **C1**. Thermal ellipsoids are drawn at 30% probability level. Crystallized methanol and all hydrogen atoms have been omitted for clarity. Selected bond lengths (Å): Ni(1)–O(1) = 2.071(3), Ni(1)–N(2) = 2.095(3), Ni(1)–N(1) = 2.095(3), Ni(1)–N(5) = 2.106(2), Ni(1)–N(4) = 2.112(3), Ni(1)–Cl(1) = 2.4668(1). Selected bond angles (°): O(1)–Ni(1)–N(2) = 169.40(2), O(1)–Ni(1)–N(1) = 90.54(1), N(2)–Ni(1)–N(1) = 79.36(1), O(1)–Ni(1)–N(5) = 94.29(2), N(2)–Ni(1)–N(5) = 84.32(1), N(1)–Ni(1)–N(5) = 99.60(1), O(1)–Ni(1)–N(4) = 85.25(2), N(2)–Ni(1)–N(4) = 104.79(1), N(1)–Ni(1)–N(4) = 175.66(1), N(5)–Ni(1)–N(4) = 79.73(1), O(1)–Ni(1)–Cl(1) = 91.97(8), N(2)–Ni(1)–Cl(1) = 91.08(7), N(1)–Ni(1)–Cl(1) = 88.97(7), N(5)–Ni(1)–Cl(1) = 169.32(7), N(4)–Ni(1)–Cl(1) = 92.20(8).

O(1)–Ni(1)–Cl(2) = 86.19(9); O(1)–Ni(1)–Cl(1) = 91.28(9). The axial position is occupied by the imidazole donor nitrogen which also formed angles 111.29(13)°, 100.71(10)°, 100.79(9)° and 80.97(12)° with donors on the tetragonal plane. A free methanol molecule was observed in the crystal lattice of **C4**. Angle between the two chlorides, Cl(1)–Ni(1)–Cl(2), is 157.75(4)°. Generally, the distances between Ni center and the O or N atoms are similar to those found in **C1**, while the Ni–Cl bond lengths found in **C4** (Ni(1)–Cl(1) = 2.3370(9) Å; Ni(1)–Cl(2) = 2.3591(9) Å) are slightly shorter compared to observed value for **C1** (2.4668(9) Å). In **C4**, the dihedral angle between the two phenyl rings (C9–C10–C11–C12–C13–C14 and C15–C16–C17–C18–C19–C20) and the imidazole ring (N2–C6–N3–C8–C7) are 61.1° and 19.8°, respectively.

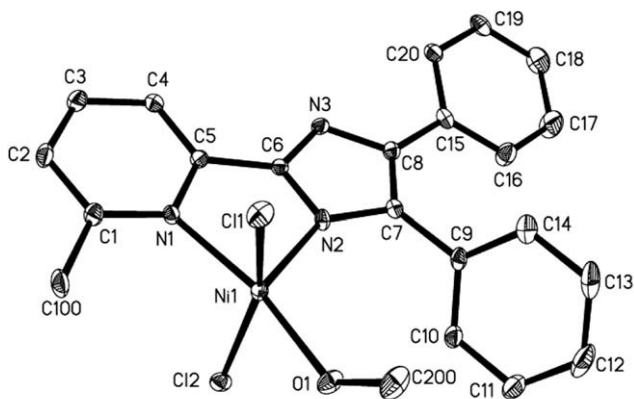


Fig. 2. Molecular structure of complex **C4**. Thermal ellipsoids are shown at the 30% probability level. Hydrogen atoms and methanol solvent have been omitted for clarity. Selected bond lengths (Å): Ni(1)–O(1) = 2.013(3), Ni(1)–N(2) = 2.014(3), Ni(1)–N(1) = 2.075(3), Ni(1)–Cl(1) = 2.3370(11), Ni(1)–Cl(2) = 2.3591(1). Selected bond angles (°): O(1)–Ni(1)–N(2) = 111.29(1), O(1)–Ni(1)–N(1) = 167.73(12), N(2)–Ni(1)–N(1) = 80.97(1), O(1)–Ni(1)–Cl(1) = 91.28(9), N(2)–Ni(1)–Cl(1) = 100.71(1), N(1)–Ni(1)–Cl(1) = 86.79(9), O(1)–Ni(1)–Cl(2) = 86.19(9), N(2)–Ni(1)–Cl(2) = 100.79(9), N(1)–Ni(1)–Cl(2) = 91.02(9), Cl(1)–Ni(1)–Cl(2) = 157.75(4).

Single crystals of **C5** were obtained by layering diethyl ether on the methanol solution of the complex. The molecular structure is shown in Fig. 3. Coordination of each nickel center can be described as distorted trigonal bipyramidal. Each nickel center is coordinated to two nitrogen atoms, one terminal chloride and two bridging chlorides. The distance between nickel and the terminal chloride (Ni(1)–Cl(2)) is 2.3429(2) Å, while the bond lengths between Ni and the bridged chlorides differ: (Ni(1)–Cl(1) = 2.3140(12) Å and Ni(1)–Cl(1A) = 2.4466(18) Å). The bridging ring is planar with a Ni(1)–Ni(1A) distance of 3.568 Å and located approximately perpendicular to both chelating rings with dihedral angles of 90.7° on either sides.

Crystals of **C8** obtained as brown blocks were grown by slow diffusion of diethyl ether into DMF solution of the complex (Fig. 4). One DMF molecule was found to be hydrogen bonded to the imidazole proton was. The nickel center has a distorted tetrahedral coordination environment consisting to two ligand donor nitrogen and the two chloride atoms. The pyridyl ring (C2–C3–C4–C5–N1–C1) is almost co-planar with the phenanthrene rings (C6–N3–C7–C8–N2) with dihedral angle 1.08°. The Ni–N bond lengths (Ni(1)–N(1) = 2.022(3) Å; Ni(1)–N(2) = 1.996(3) Å) are almost similar to those observed in **C4**. The two Ni–Cl lengths (Ni(1)–Cl(1) = 2.2404(9) Å, Ni(1)–Cl(2) = 2.1873(9) Å) are slightly different, but shorter than those in **C4** (2.3370(9) and 2.3591(9) Å). Comparison of the structures of **C4** and **C8** reveals that the two nickel centers possess only a slight difference in steric properties. Thus, it is probable that the structural difference and difference in their catalytic performances are influenced by steric effects inherent in the respective ligands.

5.4. Norbornene polymerization

To study the trends with influences of reaction parameters on catalytic performance of norbornene polymerization, the catalyst precursor **C4** was typically used. Increasing the monomer concentrations with fixed amount of **C4** (i.e. increase in M/Ni ratio) resulted in a dramatic increase of catalytic activity (Table 2). Activity increase up to 3.78×10^6 g PNB/(mol Ni h) was observed for M/Ni ratio of 32000 from the value of 1.93×10^5 g PNB/(mol Ni h) for M/Ni ratio of 4000 (Table 2, Entry 1 versus Entry 4). Meanwhile, higher molecular weight and broader molecular weight polydispersity were obtained with the elevation of the monomer concentration (Table 2, Entries 1–4).

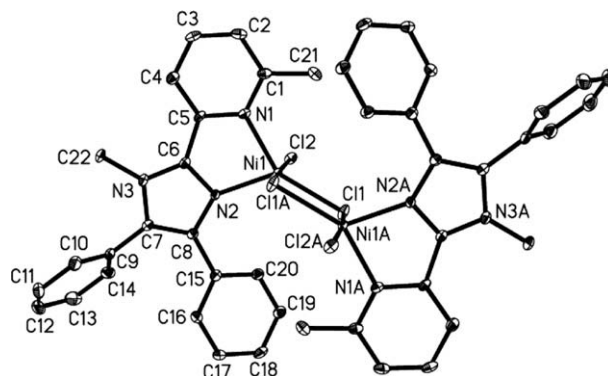


Fig. 3. Molecular structure of complex **C5**. Thermal ellipsoids are shown at the 30% probability level. All hydrogen atoms and most atomic labels for the second complex unit have been omitted for clarity. Selected bond lengths (Å): Ni(1)–N(2) = 2.012(3), Ni(1)–N(1) = 2.035(3), Ni(1)–Cl(1) = 2.3140(1), Ni(1)–Cl(2) = 2.3429(2), Ni(1)–Cl(1A) = 2.4466(2). Selected bond angles (°): N(2)–Ni(1)–N(1) = 80.92(1), N(2)–Ni(1)–Cl(1) = 130.38(1), N(1)–Ni(1)–Cl(1) = 147.42(1), N(2)–Ni(1)–Cl(2) = 97.23(1), N(1)–Ni(1)–Cl(2) = 91.42(1), Cl(1)–Ni(1)–Cl(2) = 92.76(5), N(2)–Ni(1)–Cl(1A) = 91.05(1).

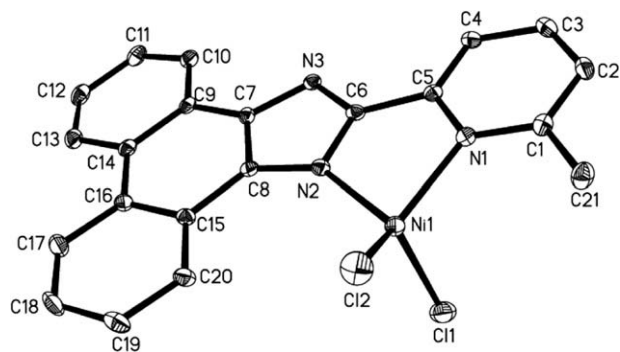


Fig. 4. Molecular structure of complex **C8**. Thermal ellipsoids are shown at the 30% probability level. Hydrogen atoms and the hydrogen bonded DMF have been omitted for clarity. Selected bond lengths (Å): Ni(1)–N(2) = 1.996(3), Ni(1)–N(1) = 2.022(3), Ni(1)–Cl(2) = 2.1873(1), Ni(1)–Cl(1) = 2.2404(1). Selected bond angles (°): N(2)–Ni(1)–N(1) = 82.38(1), N(2)–Ni(1)–Cl(2) = 118.81(8), N(1)–Ni(1)–Cl(2) = 127.97(8), N(2)–Ni(1)–Cl(1) = 104.53(8), N(1)–Ni(1)–Cl(1) = 97.65(8), Cl(2)–Ni(1)–Cl(1) = 118.34(4).

Table 2
Effect of norbornene concentration on activity of **C4**.^a

Entry	M/Ni	PNB (g)	Yield (%)	Activity ^b	M_w^c	M_w/M_n
1	4000	0.193	26.6	1.93	5.43	2.06
2	8000	0.412	27.3	4.12	9.01	2.33
3	16000	1.38	45.7	13.8	20.8	3.05
4	32000	3.78	62.0	37.8	23.3	3.36

^a Condition: 2.0 μmol **C4**; MAO/Ni = 2000; total solution volume 10 mL; 30 min; 20 °C.

^b 10⁵ g PNB/(mol Ni h).

^c 10⁵ g/mol.

The results on effect of reaction temperatures are presented in Table 3. The catalytic system displayed good activity over the studied range of reaction temperatures and the reaction temperature showed limited influence on the catalytic activities. The catalytic activities increase initially with temperature from 0 to 20 °C and reach a maximum around 20 °C. However, as reaction temperature increases from 20 to 80 °C, the activity of the catalyst decreases gradually. It is noteworthy that the molecular weight (M_w) continually decreased coupled with narrowing molecular weight polydispersity (M_w/M_n) at increasing reaction temperature (Table 3, Entries 1–5). Nickel β-diketiminates [45] and (benzamidinato)(acetylacetonato) nickel complexes [46] were found to exhibit higher productivities and higher polymer molecular weights at reducing temperatures, but this is in direct contrast with behaviour of anilido-imino nickel [29] for which trigger mechanism [37] was proposed.

The polymerization data for **C1–C9** are presented in Table 4. The coordination environment obviously has effect on the catalytic performances of the activated complexes. The bis-ligand complexes, **C1–C3**, presented lower productivity results compared to

Table 3
Influence of reaction temperatures on the activity of complex **C4**.^a

Entry	T (°C)	PNB (g)	Yield (%)	Activity ^b	M_w^c	M_w/M_n
1	0	0.650	44.0	6.50	12.7	2.42
2	20	0.896	60.6	8.96	9.01	2.33
3	40	0.490	33.2	4.90	5.61	2.16
4	60	0.455	30.8	4.55	3.88	1.90
5	80	0.388	26.3	3.88	3.17	1.75

^a Conditions: 2.0 μmol **C4**; MAO Al/Ni = 2000; Norbornene/Ni = 8000; total solution volume 10 mL, 30 min.

^b 10⁵ g PNB/(mol Ni h).

^c 10⁵ g/mol.

the mono-ligand precursors **C4–C6** (Entries 1–3 versus Entries 4–6, Table 4). This is probably as a result of less favourable generation of active components due to the number of coordination sites already claimed by the four N donors of the ligands. Moreover, broader molecular weight distributions were obtained with **C1–C3** in comparison with those of **C4–C6** (Entries 1–3 versus Entries 4–6, Table 4).

Complex **C8** ($R_1 = \text{Me}$) showed higher activity than **C7** ($R_1 = \text{H}$) (Entry 8 versus Entry 7, Table 4), which indicates that the incorporation of a methyl group on the six-position of the pyridyl ring in the complex caused slightly higher activity together with comparable molecular weight and molecular weight distribution (Entry 8 versus Entry 7, Table 4).

Comparison of the productivity of **C1** ($R_1 = R_2 = \text{H}$) with **C2** ($R_1 = \text{H}$, $R_2 = \text{Me}$) or **C4** ($R_1 = R_2 = \text{H}$) with **C5** ($R_1 = R_2 = \text{Me}$) reveal that the introduction of a methyl group on the N atom of imidazole leads to a decrease in the catalytic activity (Entry 1 versus Entry 2, or Entry 4 versus Entry 5, Table 4). Complexes **C1** and **C4** containing N–H group showed higher activities than their N-alkylated analogues **C2** and **C5**. Tentatively, these results suggest that N–H functionality is essential for high activity with this ligand system, which could be caused by their deprotonation to give anionic amide ligands when activated by MAO. The anionic amide ligands could be free or form N–Al species (anion–cation pair) to increase their catalytic activity. The observation is in agreement with our previous result in ethylene polymerization catalyzed by (2-benzimidazolyl)pyridyl nickel systems [44].

Complexes **C8** containing phenanthrene group exhibited much lower activity than its 4,5-diphenyl analogue **C4**, which may be attributed to the fact that the two steric bulky phenyl groups can flexibly protect the active species from **C4**. However, the bulky phenanthrene group is rigid and tends to be coplanar with the imidazole ring, and thus support relatively less steric hindrance to protect the active species from **C8**.

Additionally, the variation of heteroatoms in the five-membered donor ring exhibited influence on the catalytic performance. Complex **C9** containing an oxazole ring showed higher activity than **C7** bearing an imidazole ring under the same reaction conditions (Entry 9 versus Entry 7, Table 4). Higher activity on reduction of donor capacity of the five-membered ring donor nitrogen is implied in both cases and agrees with the literature findings [47]. It is interesting to note that the bromide complexes yielded obvious higher molecular weight polymers and wider molecular weight distributions relative to their chloride counterparts (Entry 1 versus Entry 3, Entry 4 versus Entry 6, Table 4).

5.5. ¹³C NMR characterization of polynorbornene

Two representative samples of polynorbornenes obtained in the current experiments were characterized by solid state ¹³C NMR

Table 4
Activities of complexes **C1–C9** for the polymerization of norbornene.^a

Entry	Cat.	PNB (g)	Yield (%)	Activity ^b	M_w^c	M_w/M_n
1	C1	0.403	27.3	4.03	1.53	3.01
2	C2	0.393	26.6	3.93	5.25	2.70
3	C3	0.539	32.5	5.39	16.8	4.12
4	C4	0.896	60.6	8.96	9.01	2.33
5	C5	0.562	38.1	5.62	7.91	1.52
6	C6	0.679	46.0	6.79	11.5	2.62
7	C7	0.353	23.9	3.53	12.9	2.24
8	C8	0.427	28.9	4.27	12.6	2.34
9	C9	0.423	28.6	4.23	10.7	2.15

^a Condition: 2.0 μmol precursors; MAO/Ni = 2000; Norbornene/Ni = 8000; total solution volume 10 mL; 30 min; 20 °C.

^b 10⁵ g PNB/(mol Ni h).

^c 10⁵ g/mol.

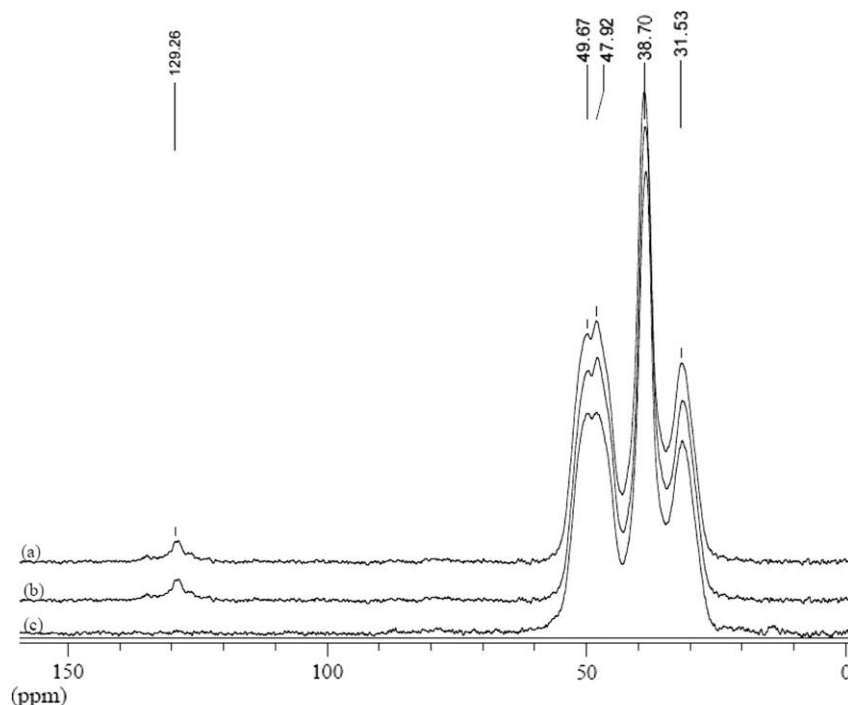


Fig. 5. Solid state ^{13}C NMR spectra of polynorbornenes obtained by **C4** (a), **C5** (b) and literature catalyst (c)¹².

measurements. Main signals occurred in the ranges of 50 ppm through 30 ppm with peaks at 48.5, 38.8 and 31.7 ppm for samples (Entries 4 and 5, Table 4) obtained by **C4** (Fig. 5a) and **C5** (Fig. 5b), however, surprisingly the observable signals around the 130 ppm region indicated C=C bonds remaining in the polymeric samples. In fact, two samples are with relative narrow molecular weight distributions, and it could be figured out that the impurity or by-product of polymers appeared. In another word, the resultant polymers in norbornene polymerization are unique polymers instead of combined polymers. Therefore, there are double bonds remaining in resulting polymers, and the double bonds could only occurred through partly happened ring-open metathesis polymerization of norbornene.

To approve this point, the solid state ^{13}C NMR of polynorbornene obtained according to our previous work (Entry 4 of Table 3 of literature [12]) is carefully investigated, and its spectrum appeared as Fig. 5c. It is no doubt that the polynorbornene through vinyl-type polymerization do not have any C=C bond, though such polynorbornene had wide molecular weight distributions [12].

According to the comparisons of the solid state ^{13}C NMR spectra, the polynorbornenes were obtained through mainly vinyl-type and minor ring-opening metathesis polymerization of norbornene. The nature of blocked polymer is proposed on the base of the unimodal GPC curves and yet narrow PDIs of obtained polymers. The resultant polynorbornenes would be new type blocked polymers with potential advantage of having melting points if the C=C bonds in polymer chain could be reductive and foldable. Experiments pertaining to the ratios and possibility of tuning the ratios would be undergoing.

6. Conclusions

A series of new nickel complexes bearing 2-(4,5-diphenyl-imidazol-2-yl)pyridines or 2-(pyridin-2-yl)phenanthroimidazoles/oxazole was synthesized and fully characterized. Reaction of **L1** and **L3** with nickel dihalides selectively formed blue, bis-ligated

complexes, while mono-ligated complexes were obtainable from **L2**, **L4** and **L5–L7**. Moreover, X-ray analysis revealed that slight variations on ligand structures informed definite preference of coordination geometry about the nickel centers from tetrahedral structure, through trigonal bipyramid and square pyramid to octahedral assemblies. The tetrahedral structure of **C8** showed that the phenanthro-derived ligand formed their own class of robust donor ability; an indication of significant difference in steric attribute of this group of ligands.

In the presence of MAO as cocatalyst, these nickel systems showed good to high activities for norbornene polymerization. The bis-chelated nickel complexes (**C1**, **C2** and **C3**) showed relatively lower catalytic activities with broader molecular weight distributions than their mono-ligand counterparts (**C4**, **C5** and **C6**). Presence of a protective methyl group ortho- to pyridyl donor nitrogen generally improved catalytic productivity. Higher activity with less donating oxazole ring relative to imidazole was observed. The polynorbornenes obtained in current system would be new type blocked polymers through mainly vinyl-type and minor ring-opening metathesis polymerization of norbornene.

Acknowledgements

This work was supported by NSFC No. 20674089. A.O.E. is grateful to the Chinese Academy of Science (CAS) and The Academy of Science for The Developing World (TWAS) for the Postgraduate Fellowships.

Appendix A. Supplementary material

CCDC 714491, 714492, 714493 and 714494 contain the supplementary crystallographic data for **C1**, **C4**, **C5** and **C8**. These data can be obtained free of charge from The Cambridge Crystallographic Data Centre via www.ccdc.cam.ac.uk/data_request/cif. Supplementary data associated with this article can be found, in the online version, at [doi:10.1016/j.ica.2009.02.026](https://doi.org/10.1016/j.ica.2009.02.026).

References

- [1] A.W. Andersen, N.G. Merklung, US Patent 2721189, to DuPont, Chem. Abstr. 50 (1954) 3008i.
- [2] R.H. Grubbs, *Tetrahedron* 60 (2004) 7117.
- [3] R.R. Schrock, *Angew. Chem., Int. Ed.* 45 (2006) 3748.
- [4] R.H. Grubbs, *Angew. Chem., Int. Ed.* 45 (2006) 3760.
- [5] G. Sartori, F.C. Ciampelli, N. Cameli, *Chim. Ind. (Milan)* 45 (1963) 1478.
- [6] B.L. Good, in: B. Rieger, L.S. Baugh, S. Kacker, S. Striegler (Eds.), *Late Transition Metal Polymerization Catalysts*, Wiley-VCH, Weinheim, 2003, p. 101.
- [7] C. Janiak, P.G. Lassahn, *J. Mol. Catal. A: Chem.* 166 (2001) 193.
- [8] C. Janiak, P.G. Lassahn, *Macromol. Rapid Commun.* 22 (2001) 479.
- [9] M. Arndt, I. Beulich, *Macromol. Chem. Phys.* 199 (1998) 1221.
- [10] S. Ahmed, S.A. Bidstrup, P.A. Kohl, P.J. Ludovice, *J. Phys. Chem. B* 102 (1998) 9783.
- [11] B.S. Heinz, F.P. Alt, W. Heiz, *Macromol. Rapid Commun.* 19 (1998) 251.
- [12] W.-H. Sun, H. Yang, Z. Li, Y. Li, *Organometallics* 22 (2003) 3678.
- [13] H. Yang, W.-H. Sun, F. Chang, Y. Li, *Appl. Catal. A* 252 (2003) 261.
- [14] H. Yang, Z. Li, W.-H. Sun, *J. Mol. Catal. A* 206 (2003) 23.
- [15] W.-H. Sun, H.-J. Yang, Z.-L. Li, *Chin. Patent* 02 1 263 18.3, 2002.
- [16] X. Mi, Z. Ma, N. Cui, L. Wang, Y. Ke, Y. Hu, *J. Appl. Polym. Sci.* 88 (2003).
- [17] X.-F. Li, Y.-S. Li, *J. Polym. Sci. Part A: Polym. Chem.* 40 (2002) 2680.
- [18] C. Mast, M. Krieger, K. Dehnicke, A. Greiner, *Macromol. Rapid Commun.* 20 (1999) 232.
- [19] Q. Wu, Y.-Y. Lu, *J. Polym. Sci. Part A: Polym. Chem.* 40 (2002) 1421.
- [20] F. Chang, D. Zhang, G. Xu, H. Yang, J. Li, H. Song, W.-H. Sun, *J. Organomet. Chem.* 689 (2004) 936.
- [21] D. Zhang, S. Jie, H. Yang, F. Chang, W.-H. Sun, *Chin. J. Polym. Sci.* 23 (2005) 619.
- [22] J. Hou, W.-H. Sun, D. Zhang, L. Chen, W. Li, D. Zhao, H. Song, *J. Mol. Catal. A* 231 (2005) 221.
- [23] D. Zhang, S. Jie, T. Zhang, J. Hou, W. Li, D. Zhao, W.-H. Sun, *Acta Polym. Sinica* 5 (2004) 758.
- [24] W. Zhang, W.-H. Sun, S. Zhang, J. Hou, K. Wedeking, S. Schultz, R. Frohlich, H. Song, *Organometallics* 25 (2006) 1961.
- [25] Q.-S. Shi, W.-W. Zuo, *Chin. J. Polym. Sci.* 26 (2008) 561.
- [26] N.H. Tarte, H.Y. Cho, S.I. Woo, *Macromolecules* 40 (2007) 8162.
- [27] Y. Wang, S. Lin, F. Zhu, H. Gao, Q. Wu, *Eur. Polym. J.* 44 (2008) 2308.
- [28] F.-B. Han, Y.-L. Zhang, X.-L. Sun, B.-G. Li, Y.-H. Guo, Y. Tang, *Organometallics* 27 (2008) 1924.
- [29] H. Gao, J. Zhang, Y. Chen, F. Zhu, Q. Wu, *J. Mol. Catal. A* 240 (2005) 178.
- [30] J. Hou, S. Jie, W. Zhang, W.-H. Sun, *J. Appl. Polym. Sci.* 102 (2006) 2233.
- [31] Q. Shi, S. Jie, S. Zhang, H. Yang, W.-H. Sun, *Macromol. Symp.* 260 (2007) 74.
- [32] X. Meng, G.R. Tang, G.-X. Jin, *Chem. Commun.* (2008) 3178.
- [33] W.-G. Jia, Y.-B. Huang, Y.-J. Lin, G.-X. Jin, *Dalton Trans.* (2008) 5612.
- [34] F. Blank, C. Janiak, *Coord. Chem. Rev.* 253 (2009) 827.
- [35] T.F.A. Haselwandel, W. Heitz, *Macromol. Rapid Commun.* 18 (1997) 689.
- [36] M.C. Sacchi, M. Sonzogni, S. Losio, F. Forlini, P. Locatelli, I. Tritto, M. Licchelli, *Macromol. Chem. Phys.* 202 (2001) 2052.
- [37] M. Ystenes, *Makromol. Chem. Macromol. Symp.* 66 (1993) 71.
- [38] E.A. Steck, A.R. Day, *J. Am. Chem. Soc.* 65 (1943) 452.
- [39] K. Wang, L. Gao, G. Bai, L. Jin, *Inorg. Chem. Commun.* 5 (2002) 841.
- [40] K. Mizuno, N. Kamiyama, N. Ichinose, Y. Otsuji, *Tetrahedron* 41 (1985) 2207.
- [41] C.W.C. Stein, A.R. Day, *J. Am. Chem. Soc.* 64 (1942) 2567.
- [42] W.-H. Sun, P. Hao, S. Zhang, Q. Shi, W. Zuo, X. Tang, *Organometallics* 26 (2007) 2720.
- [43] W.-H. Sun, K. Wang, K. Wedeking, D. Zhang, S. Zhang, J. Cai, Y. Li, *Organometallics* 26 (2007) 4871.
- [44] P. Hao, S. Zhang, W.-H. Sun, Q. Shi, S. Adewuyi, X. Lu, P. Li, *Organometallics* 26 (2007) 2439.
- [45] Y. Li, M. Gao, Q. Wu, *Appl. Organometal. Chem.* 21 (2007) 965.
- [46] E. Nelkenbaum, M. Kapon, M.S. Eisen, *Organometallics* 23 (2005) 2645.
- [47] J.A. Casares, P. Espinet, J.M. Martín-Alvarez, J.M. Martínez-Illarduya, G. Salas, *Eur. J. Inorg. Chem.* (2005) 3825.